Superhydrophobic micro-nano structures on silicone rubber by nanosecond laser processing

Lie Chen[1], Xing Wang[1], Tao Yang[2], Peter Bennett[1], Zhong Zheng[1], Qibiao Yang[1],Walter Perrie[3], Stuart P. Edwardson[3], Geoff Dearden[3], Dun Liu[1*]

1 Hubei Key Laboratory of Modern Manufacturing Quality Engineering, School of Mechanical Engineering, Hubei University of Technology, Wuhan, China
2 School of Naval Architecture and Navigation, Wuhan Technical College of Communications, Wuhan, China
3 Laser Group, Department of Engineering, University of Liverpool, Brownlow Street, Liverpool L69 3GQ, UK

Abstract: This paper demonstrates the laser surface modification of silicone rubber by using an economic and efficient nanosecond fibre laser directly. Surface morphology showed that micro-nano structures leading to an increase of surface roughness were formed after processing. The effect of laser power on surface wettability was investigated. The contact angle of silicone surface increased with the increase of laser fluence. The water contact angle on the treated surface reached up to ~158° with a rolling-off angle of ~3° when laser fluence reached 10 J/cm^2. When processed by laser, the silicone rubber surface roughness also increased with the increase of fluence and reaches a maximum of ~ 11 μm at a fluence of 9.5 J/cm^2. Analysis of pre and post processing surfaces suggested there were no significant compositional changes, but some structural change to the polymer chain, namely, cleavage of Si-O-Si bonds. It is thus proposed that the primary cause of such a significant increase in contact angle is due to the change in roughness. The preparation of super-hydrophobic silicone rubber could have important application in self-cleaning, anti-icing and anti-pollution.

Keywords: super-hydrophobic surface; laser processing; laser fluence; silicone rubber; surface modification

1. Introduction

Inspired by nature, superhydrophobic surfaces have attracted increasing research interest due to the wide range of applications such as fluid drag reduction, corrosion resistance, self-cleaning and oil-water separation [1,2]. The developments in designing and preparing superhydrophobic surfaces also have shown promising anti-icing performance [3,4], perhaps creating an opportunity to prevent the wings of aircraft or electrical insulators from icing[5]. Such surfaces can also be employed for liquid transportation [6]. Today, superhydrophobic surfaces can be generated by various techniques, such as templating, colloidal assembly, physical vapour deposition, chemical vapour deposition, hydrothermal, electrochemical deposition, etching, plasma treatment, and laser processing[7,8]. Among these methods, laser processing is a promising method due to its high efficiency, low waste and the ability to work with a large range of materials. Liu et al. used a picosecond laser to prepare an aluminium-based superhydrophobic surface. The effect of laser pulse number on the surface morphology and wettability of the sample was studied. And a stable

superhydrophobic aluminium surface with a contact angle of up to 165° was prepared [9]. Long et al. used a femtosecond laser to construct a regular micro-nano composite structure on the copper surface, and then modified with a solution of chemical reagent to obtain a superhydrophobic surface [10]. Liu and Jiang processed the surface of polyvinylidene fluoride by excimer laser to prepare a super-hydrophobic surface with a contact angle of up to 170° [11]. In general, laser processing has a good application prospect in the preparation of superhydrophobic surfaces.

Silicone rubber has been widely used in the power industry due to its high electrical and thermal insulation properties. Silicone rubber has excellent hydrophobicity and exhibits the ability to recover its hydrophobicity even after being polluted on the surface [12,13].These properties along with reduced surface icing means that silicone rubber insulators are widely used in high voltage transmission lines [14,15]and compared with the ceramic insulators, are easy and safe for installation, and have excellent resistance to mechanical shock [16,17]. However, to achieve suitable performance specific formulation, coatings are required for the production of the silicone rubber insulators used currently [18] while the water contact angles of coated silicone rubbers used currently are generally less than 120° [19]. Buildup of dirt over time can create a short circuit risk, therefore, in situ maintenance involving cleaning and recoating is required every 3 months or so especially in high temperature and pollution locations. This is costly and time consuming but has the potential to be improved by creating a superhydrophobic surface.

The preparation of superhydrophobic silicone rubber surfaces using laser micro-nano structuring has been investigated here. Most of the reported works prepare superhydrophobic surfaces by coating [20-22]. However, Liu fabricated a micro-nano structure, similar to a lotus leaf surface on H13 moulded steels using a high-power ultrafast picosecond laser, and then embossing silicone rubber to form the superhydrophobic surface [23]. High-cost and skill are required for these methods. In this paper, the superhydrophobic behaviour of silicone rubber surfaces prepared solely by nanosecond laser surface processing is presented. The superhydrophobic surfaces show the desired self-cleaning and anti-icing properties.

2. Experimental

2.1 Materials

Silicone rubber (PURESHI GJB-12514) sheets with a thickness of 2 mm were used for all the experiments in this paper. Prior to laser processing, these samples were cleaned with pure ethanol for 15 minutes in an ultrasonic bath and then dried.

2.2 Laser surface processing

Fig.1 shows the schematic diagram of optical device for processing silicone rubber surfaces. In fact, rubber material has a good thermal insulation property and its thermal conductivity is very small [24]. Considering the large thermal effect of long-pulsed lasers and the high cost of ultrashort pulse lasers, a nanosecond SPI fibre laser (100 W EP-Z) with a wavelength of 1064 nm was used to fabricate surface structure on the samples. A galvanometer scanning system was applied in moving the laser beam over the sample surface with nominal beam spot diameter of 50 μm. Focus position could be adjusted by lifting the platform. The laser was ensured to be focused on the sample surface by adjusting the vertical distance between the sample and the galvanometer. All experiments were conducted at ambient pressure in air.
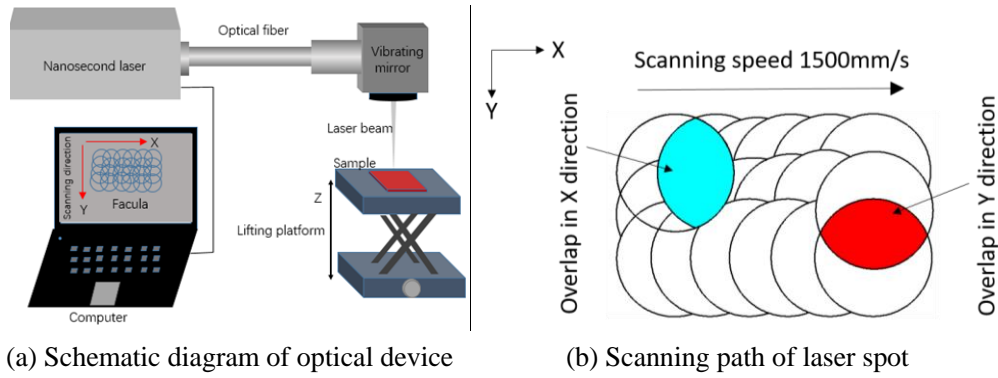
(a) Schematic diagram of optical device　　　　(b) Scanning path of laser spot

Fig.1 Schematic diagram of optical device for processing silicone rubber surfaces

Fig.1 (b) shows the scanning path of laser spot. To ensure that the sample surface could be irradiated by laser energy uniformly, a spot overlap of 70% in the X and Y directions and a repetition rate of 100 kHz were used. So the scanning speed can be calculated as blow:

$$v = (1-\delta)fD = 1500mm/s$$

where, δ is spot overlap in X direction (70%); f is repetition rate (100 kHz) and D is spot diameter (50 μm).

2.3 Surface analysis

The surface wettability of the as-received and laser processing sample surfaces was characterized by water contact angle which incorporates a camera (NAVITAR 1-6010) for image capture of the 9 μl deionized water droplets. The contact angle was obtained by analysing the droplet images using the proprietary software (Drop Meter). In order to present the morphology of the laser processing, optical inter-ferometric microscopy (BRUKER, Contour GT-K0) and scanning electron microscopy (SEM, SU8010) were used. The chemical composition of the sample surface was researched by Energy Dispersive Spectrometer (EDS) and Fourier Transform Infrared Spectrometer (FTIR) measurements.

3. Results and discussion

3.1 Superhydrophobic behaviour of silicone rubber surface

Contact angle measurement is one of the standards method to evaluate the hydrophobicity of a surface, whereby the larger the contact angle, the better the surface hydrophobicity, but hysteresis must also be taken into account to properly judge the wetting properties of a surface. Hysteresis is the difference between the advancing and receding contact angles but can also be conveniently expressed by a roll-off angle – this is the angle of tilt that needs to be applied to a surface containing a water droplet to get the water droplet to "roll off" the surface [25]. A low roll-off angle is an expression of low adhesion between droplet and surface which is essential for self-cleaning surfaces. Thus, a high contact angle (> 150°) and small rolling-off angle (< 10°) are essential for a low adhesion superhydrophobic surface [26].

The laser power has great influence on surface morphology of the irradiated surface so it should affect the surface wettability. However, an important variable of pulsed lasers is the pulse length as this changes the intensity and interaction time of the radiation with the material and hence the degree of thermal processes occurring. Fig.2 shows the change in contact angle of the processed surface as a function of pulse fluence varied from 5 J/cm² to 25 J/cm², measured at five different pulse widths
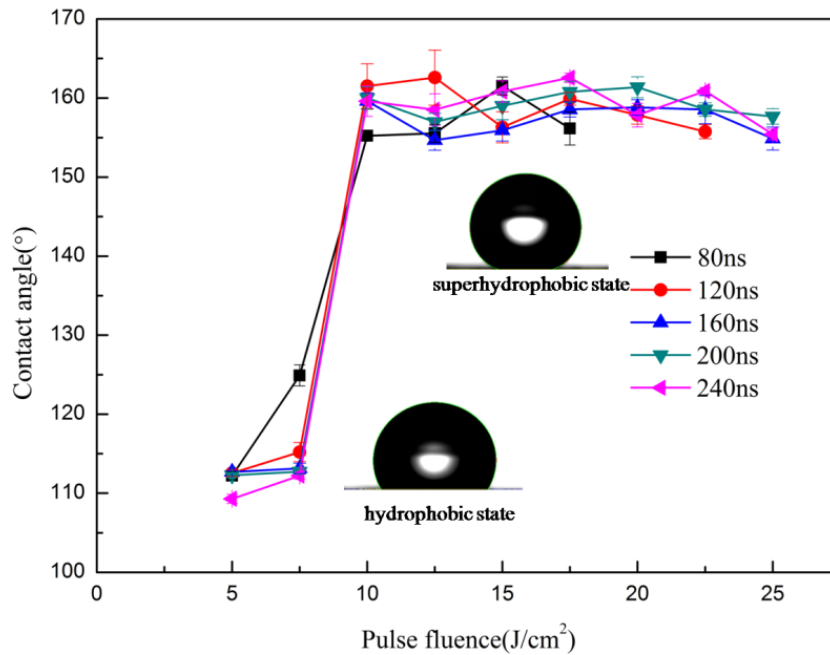
from 80 to 240 ns.

Fig.2 Effects of laser fluence and pulse widths on the contact angle of surface

It indicated that as the laser energy increases, the changes of contact angle were consistent. Contact angle of sample surface irradiated with 5 J/cm^2 and 7.5 J/cm^2 had a slight increase in contact angle. As laser power increases, the contact angle increases up to ~ 160° and reached a stable value, therefore the wettability of the sample surfaces transform into superhydrophobic from hydrophobic when the pulse fluence increases to 10 J/cm^2 and above. In view of the fact that the change of pulse width has no obvious effect on the surface wettability of the sample after laser treatment, a pulse width of 120ns was primarily employed in the subsequent experimental.

Fig.3 shows the state of water droplets on the original surface (orange) and superhydrophobic surface (white).
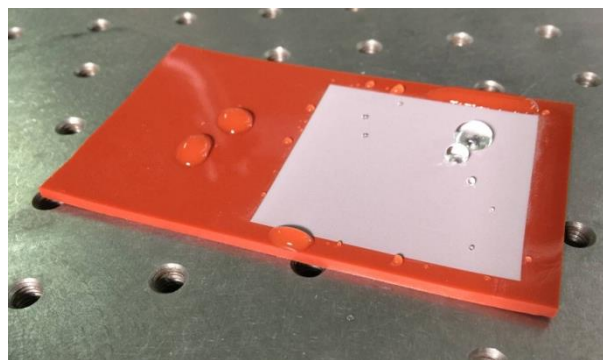

Fig.3 States of water droplet on silicone rubber, unprocessed (orange) and superhydrophobic surface (white).

Fig.4 shows the dynamic process of contact angle measurement on a silicone rubber surface irradiated with a fluence F =12.5 J/cm^2. At first, a water droplet of ~ 6 μl was suspended from a syringe (Fig.4a), then, the droplet was brought into contact with the surface by reducing the height of the syringe (Fig.4b). The water repellency of the processed surface is so high compared to the metal syringe that the droplet cannot adhere to the sample surface and appeared to slide on the measured surface as the upward force from the sample platform increased (Fig.4c). The shape of

the droplet was gradually restored as the platform was lowered (Fig.4d and e) and then completely left the surface unwetted, (Fig.4f). This indicates that the weight of the 6 µl droplet and the absence of adhesion to the sample surface were insufficient to overcome the capillary tension and adhesion forces of the water droplet to the steel of the syringe. Droplet size was increased until the weight was enough to overcome the attractive forces to the syringe – this was 9 µl and was henceforth used for all samples.
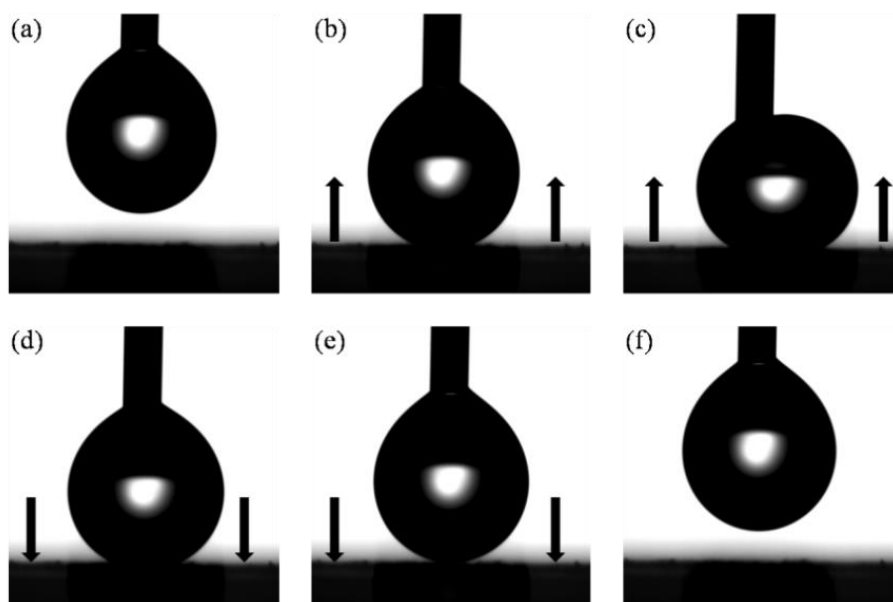

Fig.4 Low adhesion between the droplet and hydrophobic surface indicates low contact angle hysteresis. (a) ~6 µl water drop suspended on a syringe. (b) Strongly contacted with the lifting surface and (c) Sliding on the surface due to the increase of upward force. (d, e) The distortion of the droplet decreases by lowering the surface. (f) The droplet finally departed from the surface without wetting.

The rolling-off angles (RA) on original and superhydrophobic silicon rubber surface (irradiated with fluence F = 12.5 J/cm^2) were measured by applying a 9 µl water droplet to the surface . A camera recorded the event so that the angle at which the droplet rolls can be identified accurately. As can be seen from the results shown in Fig.5 (a), the contact angle (CA) on unprocessed surface was 111.4° and the rolling-off angle (RA) was larger than 90°. It means that water will be difficult to fall off from unprocessed surface without external force. Fig.5 (b) shows the water droplet rolling on a 3.1° tilted sample surface irradiated with fluence of 12.5 J/cm^2, which exhibits a good superhydrophobic property.

CA=111.4°   RA>90°

(a) Water droplet on unprocessed surface

CA=160°　　　　　　RA=3.1°
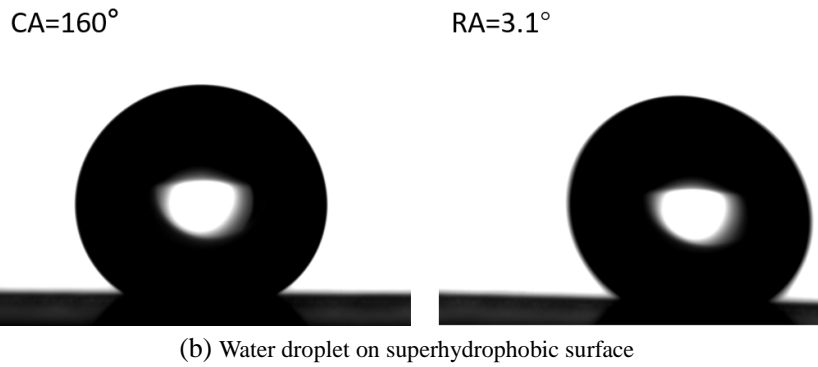
(b) Water droplet on superhydrophobic surface

Fig.5 A 9 μl water droplet rolling on unprocessed silicone rubber surface and superhydrophobic surface irradiated with fluence F =12.5 J/cm^2

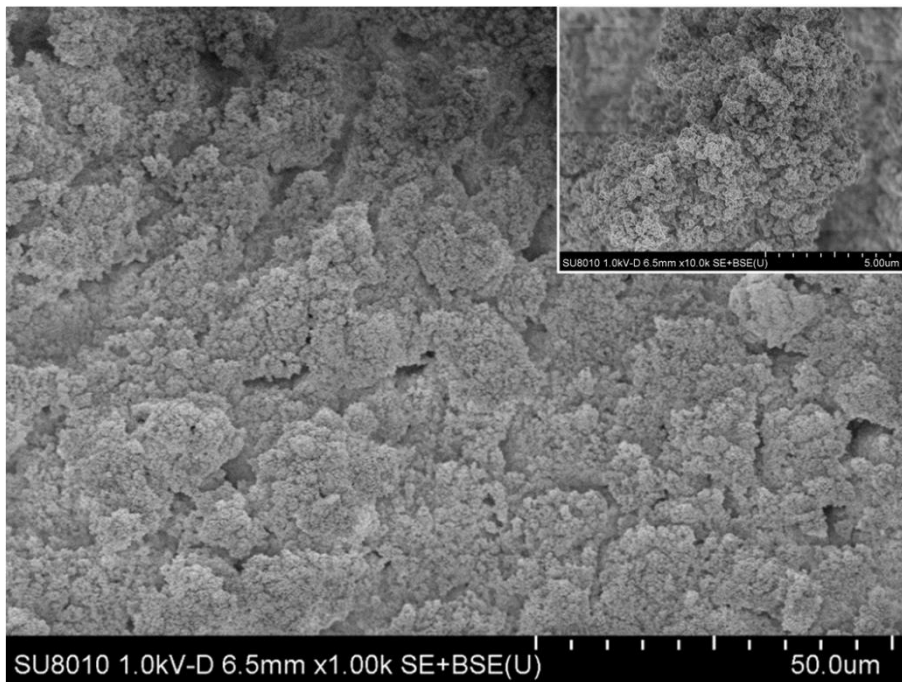## 3.2 Explanation of change in wettability

Fig.6 SEM images of laser processed surface irradiated with fluence of 12.5 J/cm^2

Fig.6 shows SEM images of the surface morphology of a silicone rubber sample irradiated at a laser fluence of 12.5 J/cm^2. The surface of the sample is superhydrophobic with a contact angle of ~ 158° and a rolling-off angle of 3°. SEM reveals that a hierarchical structure was formed on the surface after processing whereby at lower magnification, shows a fish scale type structure. Increasing in magnification, we can observe a sponge-like micro and nano structure where mastoids with a size of ~ 100 nm appear to be gathered to form irregular aggregates. Cracking, thermal ablation, vaporization and re-deposition are the likely mechanisms involved in the rearrangement of the surface matter into this complex structure. The roughness of the original surface was 0.15 μm and it was visibly clear that roughness had been increased by the laser processing surface roughness is an important factor in the wettability of a surface through limiting the contact area between droplet and surface.
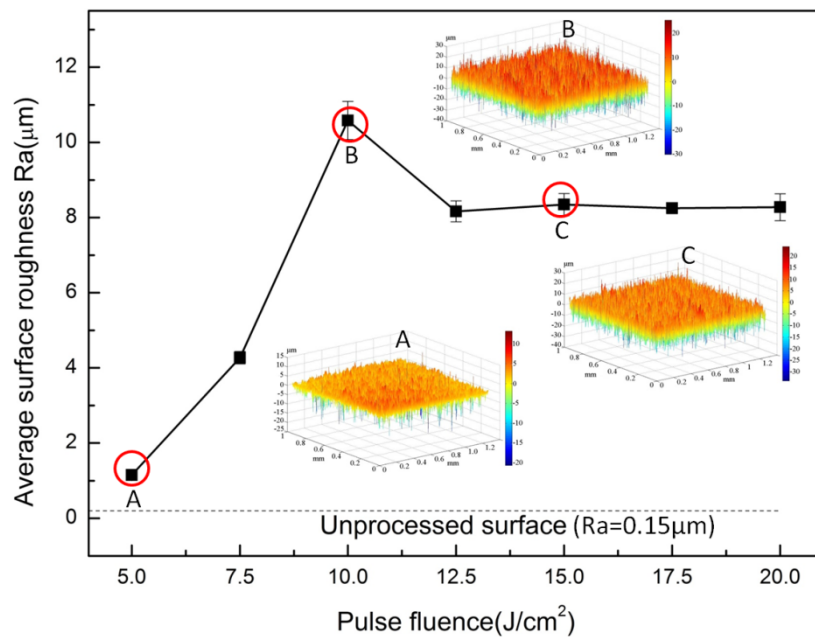
Fig.7 Surface morphology and average roughness of processed surfaces as a function of laser fluence. The insets A, B, C shows 3D profiles of a typical surface irradiated with fluences of 5, 10 and 15 J/cm^2.

To obtain more information about roughness of the surfaces, an optical microscope was used for these samples. The insets in Fig.7 presents the 3D profile of a typical surface, irradiated with fluences of 5, 10 and 15 J/cm^2. Depths for the processed structures can reach up to ~ 30 μm, but the average depth is only ~ 10 μm. Fig.7 displays the average surface roughness as a function of pulse fluence based on the three samples for each power.

The roughness of the processed surfaces for fluence up to 5 J/cm^2 was small (1.1 μm) but slightly larger than the unprocessed surface value of 0.15 μm. It is indicated that the fluence of 5 J/cm^2 is greater than the damage threshold of the silicon rubber, and rough structure was appeared. As the fluence increases, the roughness increased linearly from 5 J/cm^2 and reached a maximum value of 10.5 μm with pulse a fluence of 10 J/cm^2. With further increases of laser power, surface materials was melted and evaporated resulting in the smoothing of the processed surface with burrs gradually being reduced in scale or eliminate, such that the roughness decreased to a stable value of ~ 8.2 μm. The result shows that laser fluence has direct impacts on roughness of the processed surface.

It has been reported that the wettability of metallic surfaces textured by pulsed lasers would change over time after processing when exposed to the air and that a stable contact angle can be achieved in shorter times by the application of heat [27]. In this work, the surfaces of laser processed samples showed superhydrophobic behaviour immediately without any further processing step. This phenomenon could in principle be attributed to the modification of both surface morphology and chemistry during processing. To evaluate if there has been significant change in surface chemistry, the Energy Dispersive Spectrometer (EDS) was used to measure Carbon (C), Oxygen (O) and Silicon (Si) before after processing, Fig.8 confirms slight increases in C and O after processing whilst there is a slight reduction in Si. It is known that Adventitious Carbon (A.C) is extremely difficult to eliminate from surfaces and that it originates from the emission of carbon based materials by plant, animals, industry etc. into the atmosphere where it can, for example, be oxidized with the

aid of Ultra-Violet light, ozone and other species. A.C. is considered to comprise non-polar fatty hydrocarbon with partially oxidized polar segments resembling something akin to a fatty acid. We believe the EDS elemental data is explained by the adsorption of A.C by the processed surface which, since the processed surface has greater surface area, means increased O and C levels compared to the unprocessed surface and that the Si signal is attenuated in the processed surface also by the presence of more A.C compared to the unprocessed surface. The EDS data suggests that the dramatic reduction in wettability of the processed surface is primarily founded in a changed surface morphology, not a changed chemistry.
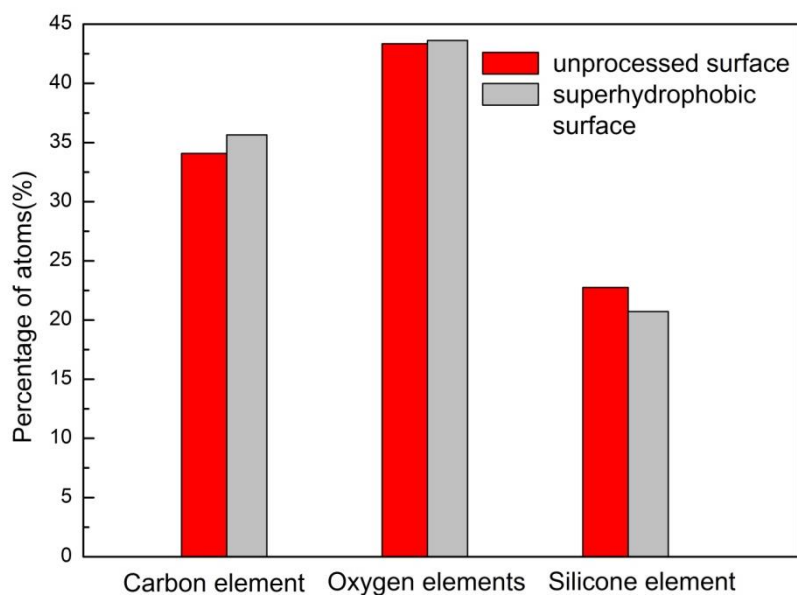

Fig.8 Comparison of Carbon, Oxygen and Silicon on unprocessed and superhydrophobic surface

3.3 Effect of laser fluence on surface morphology and chemical composition

Laser power and the resulting morphology have impacts on the wettability of the processed surface. Below, the factors are investigated, from which optimized processing parameters are presented. The same scan speed of 1500 mm/s and the beam overlap both x and y directions of 70% were applied as previously. Fig.9 presents SEM images of the effect of laser irradiation on creating micro-structures on the surface of the samples for fluences of 7.5, 10, 12.5 and 15 J/cm^2 respectively. Referring to the SEM micrographs, the surface structure shown in Fig.9a is significantly different to the rest images. At low laser fluence of 7.5 J/cm^2, the near threshold exposure was insufficient to completely remove the surface layer. Only some small holes and cracks occurred which may have been the result of evaporation and ejection of pigment mastoids, whilst most area of the surface was not ablated. Compared with the original surface, the processed surface at 7.5 J/cm^2 has a limited change in morphology. However, when processed at a laser fluence of 10 J/cm^2, a new surface texture with nano and micro scale structures was formed (Fig.9b). The surface is composed of countless tiny mastoids with a size of ~ 150 nm. As the laser fluence increases to 12.5 J/cm^2 or higher, the size of mastoids reduce to ~ 100 nm (Fig.9c and d). On the whole, surface structures shown in Fig.9 b-d were similar. The microstructure composed of mastoids increases the roughness of the sample surface and is considered the main factor for the change of wettability for silicone rubber.
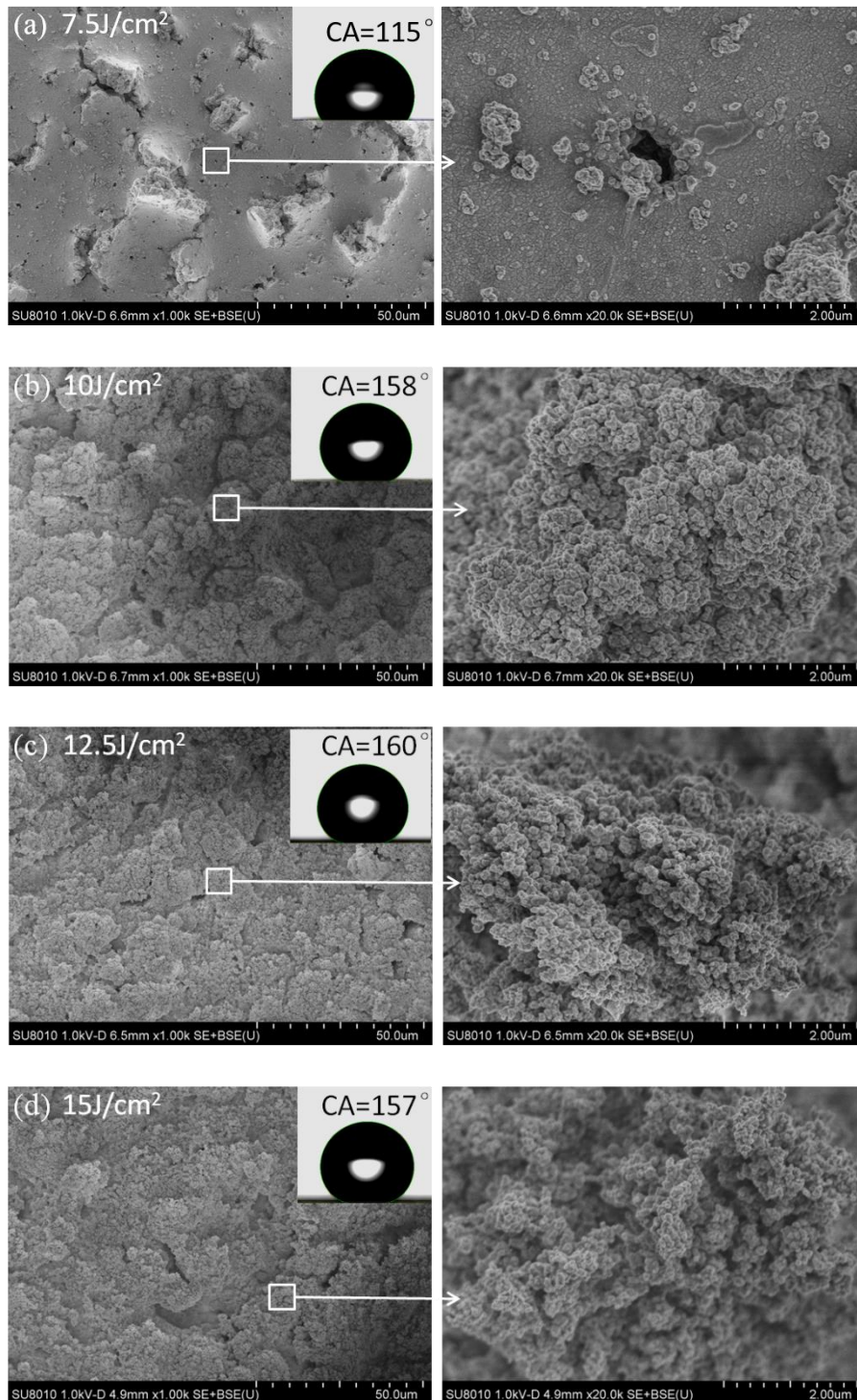
Fig.9 SEM images of laser processed surface irradiated with different laser fluence. (a)-(d) Laser fluences of 7.5, 10, 12.5, 15 J/cm^2, respectively. In (a), we see evidence of surface cracking and re-deposition while in (b) to (d), complex surface morphology develops with increasing fluence.

As mentioned earlier, EDS suggests there is no significant change in the chemistry of the surface by element type. This was further evaluated by FTIR to determine if chemical functionality or species type was changing at the surface and whether a chemical change was contributing to the wettability change. This was studied by measuring the spectra of surfaces subjected to different processing fluence as well as unprocessed. The analysis was conducted using a single reflection

diamond ATR accessory capturing twenty-five scans for each exposure, giving a very good signal to noise ratio. Six spectra (the colours of black and red represented to no exposure and 7.5 J/cm^2 are mixed up) obtained with energies ranging from zero exposure to 20 J/cm^2 with the pulse length of 120ns are shown in Fig.10. These spectra confirm that there are changes in bonding during laser processing when modifying hydrophobicity.
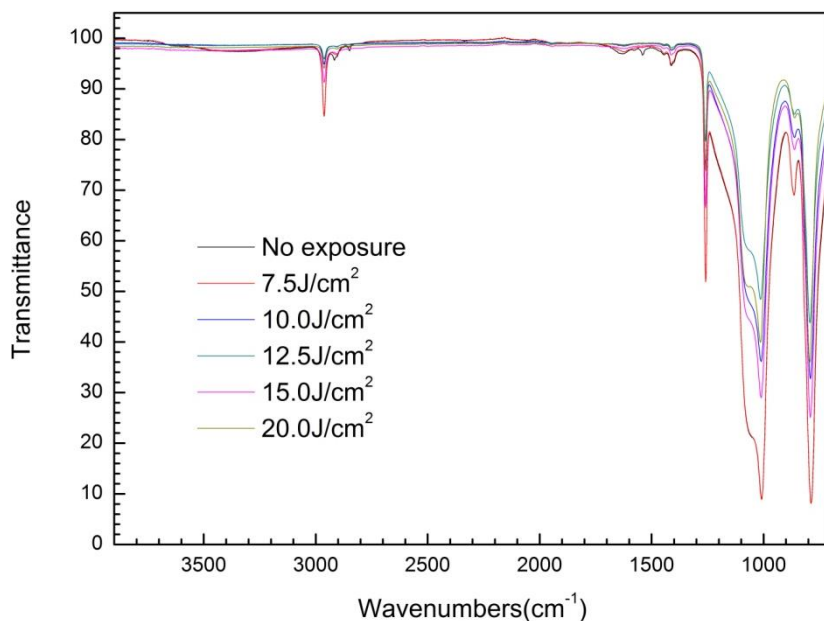

Fig.10 Spectrum of FTIR test of samples irradiated with different laser fluences from 0 to 20 J/cm^2. There are changes in observed signals with fluence in various wave number regions.

More detailed spectra are shown in Fig.11 and Fig12. Fig.11a indicates that there are small but noticeable changes in transmission with increasing exposure in the region between 2800 cm^{-1} and 3000 cm^{-1} and more significant changes in the second between 850 cm^{-1} and 1300 cm^{-1} (Fig 12a and b). The relative intensities of the CH$_3$ stretching bands at 2962 cm^{-1} and 2906 cm^{-1} change as fluence increased. The absorbance ratio was calculated by dividing the absorbance at 2906 cm^{-1} by the absorbance at 2962 cm^{-1}. As shown in Fig.11b, an increase in the Absorbance ratio indicates an increase in the absorbance at 2906 cm^{-1} compared to the absorbance at 2962 cm^{-1}. This change in the intensity at 2906 cm^{-1} could signify that the environment around the CH$_3$ functionality has changed on laser exposure to provide less steric hindrance and creating more degrees of freedom for all the CH$_3$ stretching modes.
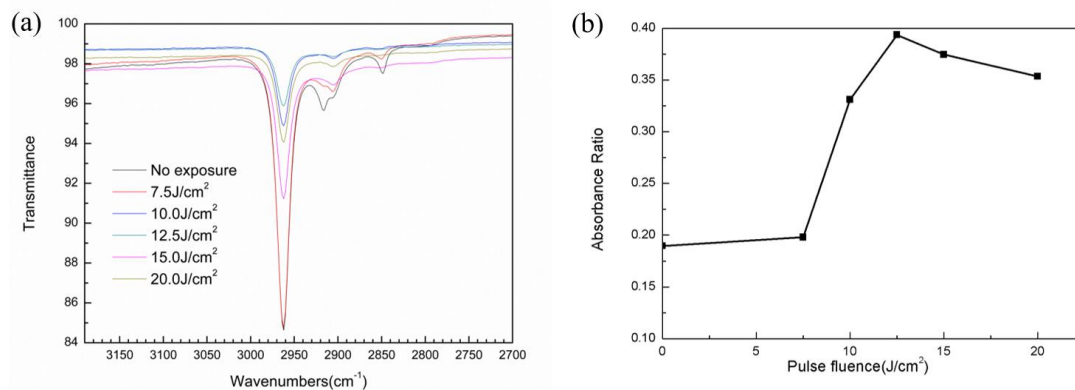
Fig.11 (a) Higher resolution spectrum between 2800cm^{-1} and 3000cm^{-1}. (b) Absorbance ratio of the band at 2906 cm^{-1} compared to the band at 2962 cm^{-1} with various fluences.
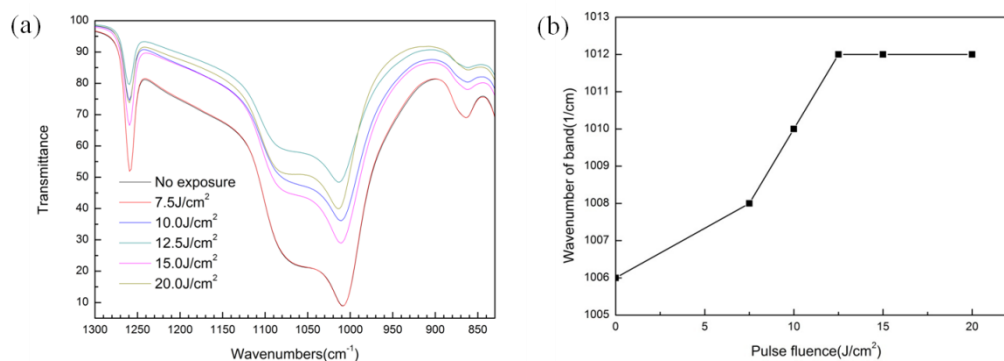

Fig.12 (a) Higher resolution spectrum between 850cm^{-1} and 1300cm^{-1}. (b) Wave number shift of the band associated with Si-O-Si at around 1010cm^{-1}.

Fig.12 (a) clearly shows that the band at 1062 cm^{-1} is changing in intensity as the exposure energy increases. There is also wave number shift of the band head at around 1010 cm^{-1} presented in Fig.12 (b). It is apparent that the exposure fluence caused a shift in the band at around 1010 cm^{-1} up to fluence of 12.5 J/cm^2 then saturates. Both these bands are associated with Si-O-Si bonds. We can tentatively conclude by examining these two areas of the spectrum that laser exposure is causing some break down of the siloxane backbone causing a shift in the Si-O-Si stretching frequencies and that this in turn facilitates easier stretching of the CH$_3$ group associated with a subsequent change in its frequencies. Since this suggests a lower molecular weight of the polymer after laser exposure with no obvious change in functionality, it again suggests that the change in wetting behaviour is due to the change in morphology and not a chemical process.

3.4 Modification of surface morphology from hydrophobic to superhydrophobic

From the previous analysis, it can be known that the chemical composition is substantially unchanged after being irradiated by the laser beam but that the morphology of the silicone rubber surface is substantially changed and this modification of surface structure was also investigated further.
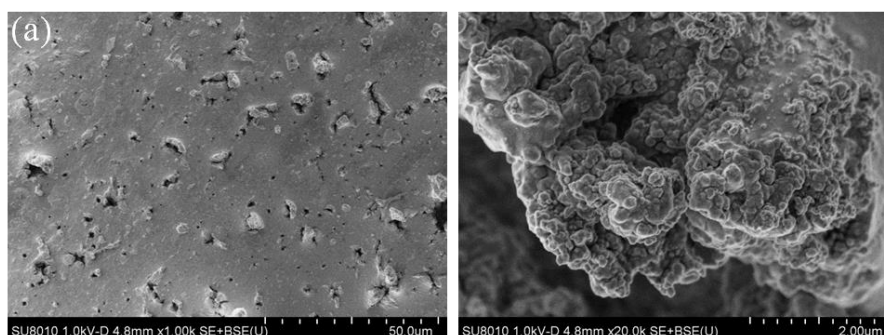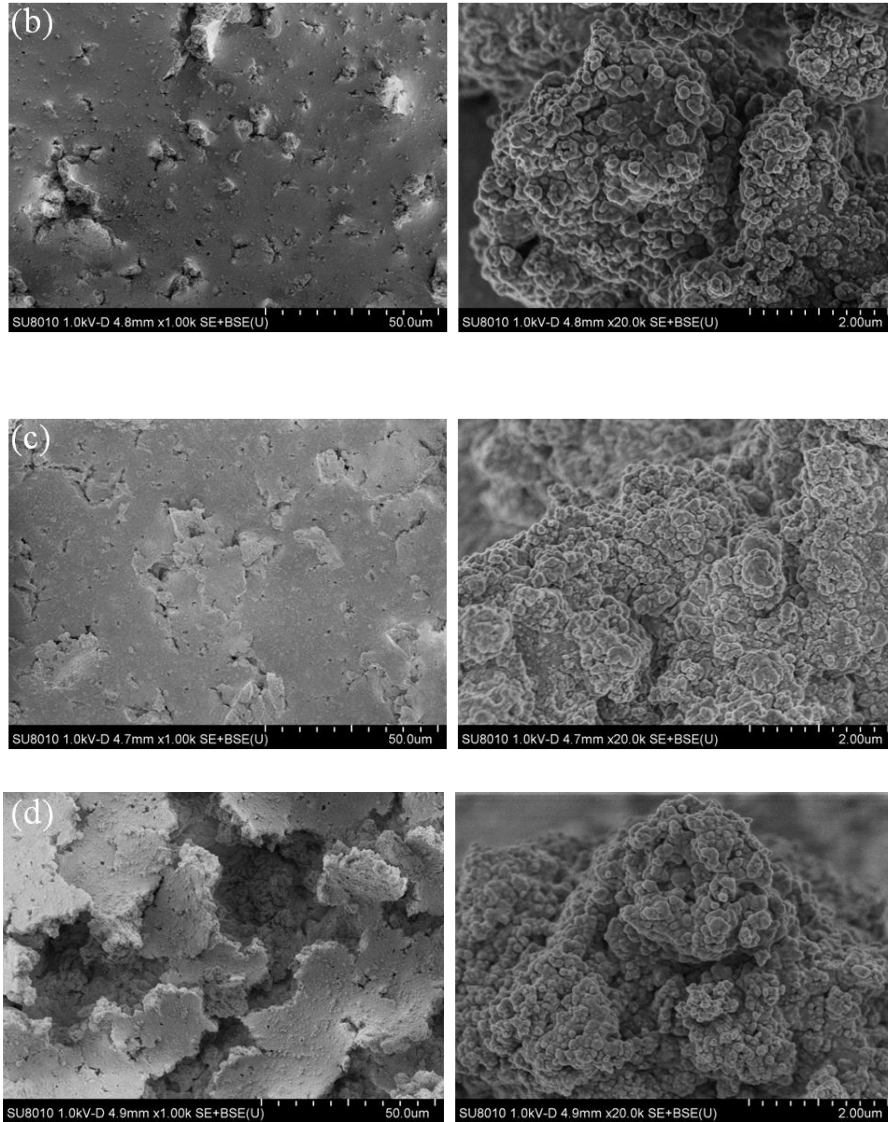
Fig.13 SEM images of laser processed surface irradiated with low laser fluence. (a)-(d) Laser fluences of 8.0, 8.5, 9.0, 9.5 J/cm^2, respectively.

Fig.13 shows SEM images taken when the silicone surface was exposed to lower fluences in the range F = 8.0-9.5 J/cm^2. From the SEM micrographs in Fig.13 (a-d) on the left, it is clear that as the laser fluence increases, the extent and intensity of surface cracking of the silicone rubber is increasing. During the process of thermal cracking, the surface roughness also increases with fluence from R_a = 4.5 μm (F = 8.0 J/cm^2) and reaches a maximum of R_a = 11 μm at a fluence of 9.5 J/cm^2. At this point, the surface of the silicone rubber appears de-adhered from the bulk and torn due to the thermal ablation. As the fluence continues to increase, the surface is further broken down into fine mastoids, forming a new surface (shown in Fig.9), which causes a decrease of surface roughness, shown in Fig.14b. In this process, the incidence of nano-mastoids on the surface increases with fluence, and gradually form a hierarchical micro-nano structure, as shown in Fig.13 (right). The trend of the surface's behaviour to water, as measured by the water contact angle is shown in Fig.14a, water contact angle as a function of pulse fluence. This is entirely consistent with the extensive formation of micro-nano structures on surface and in full agreement with the Cassie reference.
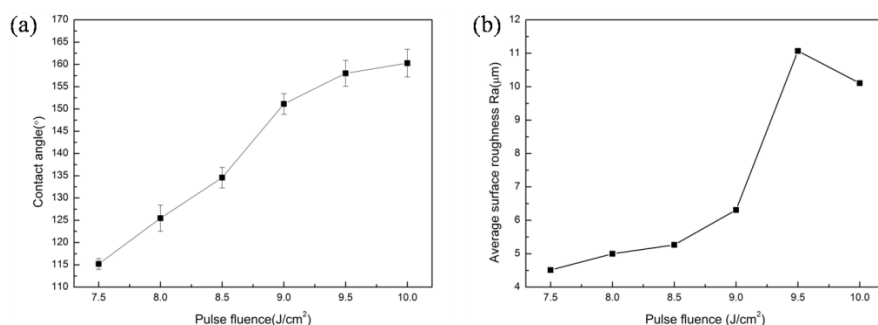
Fig.14 Surface contact angle (a) and average roughness of processed surfaces (b) as a function of laser fluence over the range from 7.5 J/cm^2 to 10 J/cm^2.

4. Conclusion

It has been shown that superhydrophobic surface can be generated on a silicone rubber by using an economic and efficient nanosecond fibre laser focused and scanned on the substrate in air without any further processing steps. Compared with metal surfaces, the silicone rubber was cracked by heat without spattering followed by the generation of new hierarchical micro-nano structures on the surface. The wettability of the processed surfaces develops from hydrophobicity to superhydrophobicity when the laser fluence reaches 10 J/cm^2 or more. The steady state contact angle is ~ 158° with small rolling-off angle of ~ 3°. Surface morphology is substantially modified whilst only physical chemical changes are observed after being irradiated with laser beam directly. Compared with the original surface, the roughness of the processed surface is increased from 4 μm to 11 μm. EDS results show a higher levels of elemental C and O and a lower level of Si on the superhydrophobic sample surfaces, most likely due to the adsorption of adventitious carbon from the air onto the larger surface area of the processed sample. On the other hand, FTIR measurements imply that Si-O-Si bonds have been cleaved, suggesting the polymer chain has been broken during NIR nanosecond ablation. The significant modification of the surface micro-structure was investigated and deemed to be the primary reason for the conversion from hydrophobic to superhydrophobic surface. During the process of thermal cracking for silicone rubber, the surface roughness increases with fluence and reaches a maximum of ~ 11 μm at a fluence of 9.5 J/cm^2. Temporal pulse length was shown to have only a minor effect on the fluence required to generate the superhydrophobic surface. This work provides a clean laser processing method with high efficiency and low cost for the preparation of superhydrophobic surfaces on silicone rubber products with potential application in self-cleaning, anti-icing and anti-pollution high voltage insulators.

References

[1]   Z. Zhang, B. Ge, X. Men, Y. Li, Mechanically durable, Superhydrophobic Coatings Prepared by Dual-layer Method for Anti-corrosion and Self-cleaning, Colloids Surfaces A Physicochem. Eng. Asp., **490**, 182-188, 2016.

[2]   F. Z. Zhang, G. M. Peng, L. M. Wang, Z. C. Guan, Influence of Environmental Temperature

on Flashover Voltage of Composite Insulator, High Volt. Eng., **36**, 1119-1123, 2010.

[3]   S. Xuan, Y.N. Zhang, Formula of Silicone Rubber Material for Composite Insulator in Power System, China Synth. Rubber Ind., **35**, 295-299, 2012.

[4]   B. Xin, J. Hao, Reversibly Switchable Wettability, Chemical Society Reviews, **39**, 769-782, 2010.

[5]   V. D. Ta, A. Dunn, T.J. Wasley, J. Li, R.W. Kay, J. Stringer, P.J. Smith, E. Esenturk, C. Connaughton, J.D. Shephard, Laser Textured Superhydrophobic Surfaces and Their Applications for Homogeneous Spot Deposition, Appl. Surf. Sci., **365**, 153-159, 2016.

[6]   D. V Ta, A. Dunn, T.J. Wasley, R.W. Kay, J. Stringer, P.J. Smith, C. Connaughton, J.D. Shephard, Nanosecond Laser Textured Superhydrophobic Metallic Surfaces and Their Chemical Sensing Applications, Appl. Surf. Sci., **357**, 248-254, 2015.

[7]   K. Siderakis, D. Agoris, S. Gubanski, Salt Fog Evaluation of RTV SIR Coatings With Different Fillers, IEEE Trans. Power Deliv., **23**, 2270-2277, 2008.

[8]   K. Siderakis, D. Agoris, Performance of RTV Silicone Rubber Coatings Installed in Coastal Systems, Electr. Power Syst. Res., **78**, 248-254, 2008.

[9]   D. Liu, Y. G. Wu, Y. T. Hu, Y. Wu, Q. B. Yang, D. Y. Lou, Z. S .Zhai, L. Chen, B. Peter, Fabrication of Super-hydrophonic Aluminum Surface by Picosecond Laser, Laser & Optoelectronics Progress, **10**, 173-181, 2016. ·

[10]   J. Y. Long, Y. C. Wu, D. W. Gong, P. X. Fan, D. F. Jiang, Femtosecond Laser Fabricated Superhydrophobic Copper Surfaces and Their Anti-icing Properties, Chinese J Lasers, **42**, 0706002, 2015.

[11]   Y. Liu, Y. J. Jiang. Super-hydrophobic Surface of Poly (Vinylidene Fluoride) Film Fast Fabricated by KrF Excimer Laser Irradiation, Chinese J of Lasers, **38**, 0106002, 2011.

[12]   Feng Shi, Xiaoxin Chen, Liyan Wang, Jia Niu, Jihong Yu, Zhiqiang Wang, Xi and Zhang, Roselike Microstructures Formed by Direct In Situ Hydrothermal Synthesis: From Superhydrophilicity to Superhydrophobicity, Chem. Mater., **17**, 6177-6180, 2005.

[13]   S. A. Seyedmehdi, H. Zhang, J. Zhu, Superhydrophobic RTV Silicone Rubber Insulator Coatings, Appl. Surf. Sci., **258**, 2972-2976, 2012.

[14]   G. Momen, M. Farzaneh, R. Jafari, Wettability Behaviour of RTV Silicone Rubber Coated on Nanostructured Aluminium Surface, Appl. Surf. Sci., **257**, 6489-6493, 2011.

[15]   G. Momen, M. Farzaneh, Survey of Micro/nano Filler Use to Improve Silicone Rubber for Outdoor Insulators, Rev. Adv. Mater., **27**, 1-13, 2011.

[16]   R. Menini, M. Farzaneh, Elaboration of Al_2O_3 /PTFE Icephobic Coatings for Protecting Aluminum Surfaces, Surf. Coat. Technol., **203**, 1941-1946, 2009.

[17]   D. Lv, J. Ou, M. Xue, F. Wang, Stability and Corrosion Resistance of Superhydrophobic Surface on Oxidized Aluminum in NaCl Aqueous Solution, Appl. Surf. Sci., **333**, 163-169, 2015.

[18]   J. Long, P. Fan, M. Zhong, H. Zhang, Y. Xie, L. Chen, Superhydrophobic and Colorful Copper Surfaces Fabricated by Picosecond Laser Induced Periodic Nanostructures, Appl. Surf. Sci., **311**, 461-467, 2014.

[19]   Q. Liu, D. Liu, Y. Yang, Research on Superhydrophobic Silicon Rubber Surface Made by High Voltage Electrospray, High Volt. Eng., **41**, 2818-2824, 2015.

[20]   C. Lin, M. Zhong, P. Fan, J. Long, D. Gong, H. Zhang, Picosecond Laser Fabrication of Large-area Surface Micro-nano Lotus-leaf Structures and Replication of Superhydrophobic

Silicone Rubber Surfaces, Chinese J. Lasers, **41**, 0903007, 2014.

[21]   S.A. Kulinich, M. Farzaneh, On Ice-releasing Properties of Rough Hydrophobic Coatings, Cold Reg. Sci. Technol., **65**, 60-64, 2011.

[22]   A. M. Kietzig, S. G. Hatzikiriakos, P. Englezos, Patterned Superhydrophobic Metallic Surfaces, Langmuir the Acs Journal of Surfaces & Colloids, **25**, 4821-4827, 2009.

[23]   X. Jiang, J. Yuan, L. Shu, Z. Zhang, J. Hu, F. Mao, Comparison of DC Pollution Flashover Performances of Various Types of Porcelain, Glass, and Composite Insulators, IEEE Trans. Power Deliv. **23**, 1183-1190, 2008.

[24]   L. Chen, J. Wang, D. Liu, Z. S. Zhai, Q. B. Yang, D. Y. Lou, B. Peter, Experimental and Mechanism Analysis of Holes Drilling on Rubber Damping Material Using Nanosecond Laser, Acta Optica Sinica, **35**, s216004, 2015.

[25]   A. Dunn, J. V Carstensen, K. L. Wlodarczyk, E. B. Hansen, J. Gabzdyl, P. M. Harrison, J. D. Shephard, D. P. Hand, Nanosecond Laser Texturing for High Friction Applications, Opt. Lasers Eng., **62**, 9-16, 2014.

[26]   M. Farzaneh, Atmospheric Icing of Power Networks, Springer Netherlands, 2008.

[27]   J. Drelich, E. Chibowski, D. D. Meng, K. Terpilowski, Hydrophilic and Superhydrophilic Surfaces and Materials, Soft Matter., **7**, 9804-9828, 2011.